

## Inspection of a Rectangular Plate Dynamics Under a Moving Mass With Varying Velocity Utilizing BCOPs

### Abstract

This research is dedicated to the inspection of a thin rectangular plate dynamic behavior traversed by an accelerated moving mass. BCOPs (boundary characteristic orthogonal polynomials) are utilized to treat the constitutive equation of plate vibration for different boundary conditions. Comprehensive parametric surveys are carried out to shed light on the effects of the plate fixities and aspect ratios as well as the moving mass weight, velocity and acceleration on the plate DAF (dynamic amplification factor). The convenience of adopting the presented solution dealing with various plate fixity cases makes it a superior approach comparing with eigenfunction expansion method.

### Keywords

accelerated moving mass, thin rectangular plate, vibration, Boundary Characteristic Orthogonal Polynomials.

Motahareh Niaz <sup>a</sup>

Ali Nikkhoo <sup>b</sup>

<sup>a</sup> Department of Civil Engineering, University of Science and Culture, Tehran, Iran. E-mail: [m.niaz@usc.ac.ir](mailto:m.niaz@usc.ac.ir)

<sup>b</sup> Department of Civil Engineering, University of Science and Culture, Tehran, Iran. Corresponding author, P. O. Box 13145-871, Tel.: +98-21-44252045, Fax: +98-21-44214750, E-mail: [nikkhoo@usc.ac.ir](mailto:nikkhoo@usc.ac.ir)

<http://dx.doi.org/10.1590/1679-78251316>

Received 28.06.2014

In revised form 19.11.2014

Accepted 26.01.2015

Available online 07.02.2015

## 1 INTRODUCTION

There are several types of civil structures and mechanical devices, which carry dynamic forces or moving loads with varying positions and magnitudes such as bridges, sleepers, cable ways, guide ways, overhead cranes, rails, road ways and run ways (Ouyang, (2011); Olsson, (1991)). Engineers also encounter the moving load dynamic problems in the analysis of rotating machinery, computer disk file memories and guided circular saws as well as decks of ships on which aircraft lands (Cifuentes, and Lalapet, (1992); Frýba, (1999); Ebrahimzadeh Hassanabadi et al. (2014a)) . Frýba (1999) has presented a comprehensive monograph on the moving load problems citing a considerable number of published researches before 1999. In contrast to the availability of a voluminous literature discussing beams acted upon by the traveling masses (Nikkhoo et al. (2007); Kiani et al.

(2009a, 2009b, 2010); Kiani and Nikkhoo (2012); Ahmadi and Nikkhoo (2014), Nikkhoo et al. (2015); Bulut and kelesoglu (2010); Zarfam et al. (2013); Eftekhari Azam et al.(2013); Ebrahimzadeh Hasanabadi et al.(2013)), vibration of plates under the action of the moving loads has so far received slight attention.

A traveling inertial load can either be simulated by the moving force or the moving mass frameworks. A moving force is a simplified definition of a traveling load wherein the inertia of the moving object is ignored. The moving mass is a realistic model of a moving load in which the inertial effects of the traveling load are considered in the problem formulations. In the aforementioned, the analytical solution to the problem would hardly exist (Frýba, (1999)). In order to handle the plate vibration problems excited by the moving loads, numerical (Wu, (2003, 2005); De Faria and Oguamanam(2004); Mohebpour et al.(2011); Esen,(2013)) or semi-analytical methods (Shadnam et al.(2001); Rofooei and Nikkhoo (2009); Ghafoori et al.(2011); Nikkhoo and Rofooei (2012); Vaseghi Amiri et al.(2013); Nikkhoo et al.(2014)) could be utilized. Amongst semi-analytical approaches, eigenfunction expansion method has been widely employed. In this regard, Shadnam et al.(2001) tackled the problem of a rectangular Kirchhoff plate vibration with simply supported edges traversed by a moving mass. Although only the vertical component of the moving mass out-of-plane acceleration was considered in their formulations, but consideration of moving load, inertial effects were reported to be crucial. The influence of the whole components of the moving mass out-of-plane translational acceleration terms have been evaluated by Nikkhoo and Rofooei (2012). Oni and Awodola (2011) and Awodola and Oni (2013) investigated the problem of a thin plate rested on a variable Winkler elastic foundation traversed by a moving force or a moving mass with simple and some other boundary conditions of the structure, respectively. They employed separation of variables method in joint with the modified method of Struble and integral transformations to solve the mathematical governing equation. Their results were indicative of the moving force inertial effects on the dynamic parameters pertinent to the understudy structure response. Vaseghi Amiri et al.(2013) explored the dynamic behavior of a rectangular Mindlin plate with different boundary conditions and patterns of moving load distribution via eigenfunction expansion method. They underlined the significance of the shear deformations for moderately thick plates. However, the main body of their parametric studies was confined to a simply supported plate. Nikkhoo et al. (2014) studied the resonance of a single span rectangular plate due to multiple opposing masses. The complex analytical handling of the plate natural mode-shapes could be mentioned as the main deficiency in utilizing the eigenfunction expansion method for non-simply supported plates.

BCOPs have been extensively used dealing with free vibration of plates with various geometries and boundary conditions. Bhat (1985) employed a set of beam orthogonal polynomials in the Rayleigh-Ritz method to calculate natural frequencies of the rectangular plates. Chakraverty (1992) and Singh and Chakraverty (1994) generated two-dimensional orthogonal polynomials to study vibration problems of plates for a variety of the plate geometries. Liew et al. (1990) took advantage of BCOPs in the free vibration analyses of the rectangular plates with different boundary conditions. The rapid convergence rate and handiness of modeling plates with arbitrary classical boundary conditions are the major benefits of this approach.

In this article, the application of BCOPs is extended to the determination of the response spectra of a thin rectangular plate excited by a traveling mass. There is a lack of investigation in the

existing literature on the plate dynamic behavior under a traveling load with varying velocity. Additionally, the previously carried out parametric surveys by different researchers are just limited to a simply supported plate. This is while a moving load in practice is more likely to have non-zero traveling acceleration. Besides, the plate boundary conditions could be a key factor in determining the plate dynamic performance. Consequently, in this article, dynamics of a rectangular plate excited by an accelerating mass is studied in detail accounting for initial mass velocity, acceleration and weight. Different plate fixities are included in the numerical examples to assess the influence of boundary conditions on the plate dynamic response. The explorations indicate that the maximum response of the plate increases with an increase in initial mass acceleration for some high initial load velocities. It is also observed that with the increase in the load acceleration, the dynamic amplification factor of the plate almost decreases.

## 2 PROBLEM DEFINITION AND FORMULATION

An elastic isotropic thin rectangular plate with arbitrary boundary conditions is assumed. This system is supposed to be undamped.  $0 \leq x \leq A$  and  $0 \leq y \leq B$  and  $-\frac{h}{2} \leq z \leq \frac{h}{2}$  describe the plate domain in  $xyz$  plane and  $(X(t), Y(t))$  designates the parametric trajectory of the moving mass as shown in Fig .1.

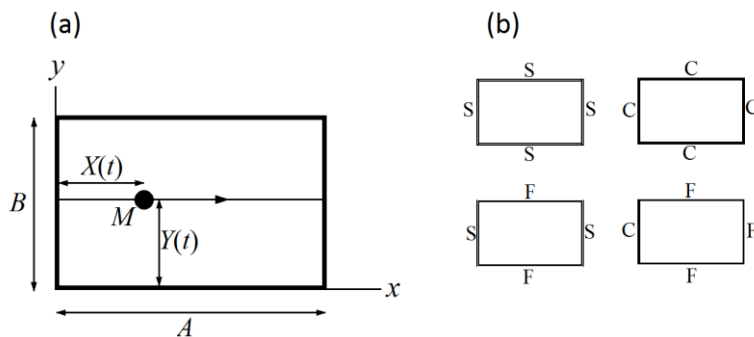


Figure 1: (a) The layout of the problem; (b) Plate boundary conditions. S, C and F, respectively, stand for simple, clamped and free edge.

The linear strains  $\varepsilon_{ij}$  due to the bending deflection  $w$  are:

$$\left\{ \begin{array}{l} \varepsilon_x = -z \frac{\partial^2 w}{\partial x^2}, \\ \varepsilon_y = -z \frac{\partial^2 w}{\partial y^2}, \\ \varepsilon_{xy} = -z \frac{\partial^2 w}{\partial x \partial y}, \\ \varepsilon_z = \varepsilon_{xz} = \varepsilon_{yz} = 0. \end{array} \right. \quad (1)$$

The principle of virtual displacements for the time-dependent case can be stated by:

$$\iiint_V \left[ \rho z^2 \left( \frac{\partial \delta w}{\partial x} \frac{\partial^3 w}{\partial x \partial t^2} + \frac{\partial \delta w}{\partial y} \frac{\partial^3 w}{\partial y \partial t^2} \right) + \rho \delta w \frac{\partial^2 w}{\partial t^2} + \delta \varepsilon_x \sigma_x + \delta \varepsilon_y \sigma_y + 2 \delta \varepsilon_{xy} \sigma_{xy} \right] dV - f \delta w = 0 \quad (2)$$

Where,  $\rho$  denotes the mass per unit volume of the plate,  $\sigma_{ij}$  signifies the stress and  $V$  stands for the plate volume and  $f$  denotes the external load. The volume integral can be written as

$$\iiint_V dV = \iint \int_{-h/2}^{h/2} dz dx dy . \text{ Therefore, Eq. (2) can be reproduced arriving at:}$$

$$\int_0^A \int_0^B \left( \delta w I_0 \frac{\partial^2 w}{\partial t^2} + \frac{\partial \delta w}{\partial x} I_2 \frac{\partial^3 w}{\partial x \partial t^2} + \frac{\partial \delta w}{\partial y} I_2 \frac{\partial^3 w}{\partial y \partial t^2} - M_x \frac{\partial^2 \delta w}{\partial x^2} - M_y \frac{\partial^2 \delta w}{\partial y^2} - 2 M_{xy} \frac{\partial^2 \delta w}{\partial x \partial y} \right) dx dy - f \delta w = 0 \quad (3)$$

in which  $h$  is the plate thickness and

$$\begin{cases} M_x = -D \left( \frac{\partial^2 w}{\partial x^2} + \nu \frac{\partial^2 w}{\partial y^2} \right) , \\ M_y = -D \left( \nu \frac{\partial^2 w}{\partial x^2} + \frac{\partial^2 w}{\partial y^2} \right) , \\ M_{xy} = -\frac{1}{6} G h^3 \frac{\partial^2 w}{\partial x \partial y} , \\ I_0 = \rho h , \\ I_2 = \frac{1}{12} \rho h^3 . \end{cases} \quad (4)$$

In Eq. (4)  $D = \frac{E h^3}{12(1-\nu^2)}$  is the plate rigidity,  $G = \frac{E}{2(1+\nu)}$  is the shear modulus,  $E$  and  $\nu$  are the plate’s modulus of elasticity and Poisson’s ratio, correspondingly. The mathematical definition of the transverse dynamic force  $f$  due to a moving mass is( Frýba, (1999)):

$$\begin{cases} f(x, y, t) = -M \left( g + \frac{d^2 w_0(t)}{dt^2} \right) , \\ w_0(t) = w(X(t), Y(t), t) . \end{cases} \quad (5)$$

$M$  and  $g$  are the mass of the moving load and acceleration of gravity in Eq. (5), respectively. In this study, the moving mass is assumed to remain connected to its supporting structure during its motion on the plate surface area. This constraint has been considered by many researchers; however in some studies, possible separation of the mass and the plate has been evaluated by monitoring the

contact force (Ebrahimpzadeh Hassanabadi et al., 2014b); this restriction has been removed in the computational process of the problem by Lee (1996) and Stăncioiu et al. (2008). The expanded version of  $\frac{d^2w_0(t)}{dt^2}$  in Eq. (5) is

$$\begin{aligned} \frac{d^2w_0}{dt^2} = & \left[ \frac{\partial^2 w}{\partial t^2} + \frac{\partial^2 w}{\partial x^2} \left( \frac{dX}{dt} \right)^2 + \frac{\partial^2 w}{\partial y^2} \left( \frac{dY}{dt} \right)^2 + 2 \frac{\partial^2 w}{\partial x \partial y} \left( \frac{dX}{dt} \right) \left( \frac{dY}{dt} \right) + 2 \frac{\partial^2 w}{\partial x \partial t} \left( \frac{dX}{dt} \right) \right. \\ & \left. + 2 \frac{\partial^2 w}{\partial y \partial t} \left( \frac{dY}{dt} \right) + \frac{\partial w}{\partial x} \left( \frac{d^2 X}{dt^2} \right) + \frac{\partial w}{\partial y} \left( \frac{d^2 Y}{dt^2} \right) \right]_{\substack{x \rightarrow X(t) \\ y \rightarrow Y(t)}} \end{aligned} \tag{6}$$

By substituting Eq. (5) and (6) into Eq. (3) the weak form of the problem becomes:

$$\begin{aligned} & \int_0^A \int_0^B \left( \delta w I_0 \frac{\partial^2 w}{\partial t^2} + D \left( \frac{\partial^2 w}{\partial x^2} + \nu \frac{\partial^2 w}{\partial y^2} \right) \frac{\partial^2 \delta w}{\partial x^2} + D \left( \nu \frac{\partial^2 w}{\partial x^2} + \frac{\partial^2 w}{\partial y^2} \right) \frac{\partial^2 \delta w}{\partial y^2} + \left( \frac{1}{3} Gh^3 \frac{\partial^2 w}{\partial x \partial y} \right) \frac{\partial^2 \delta w}{\partial x \partial y} \right) dx dy \\ & + M \left[ g + \left[ \frac{\partial^2 w}{\partial t^2} + \frac{\partial^2 w}{\partial x^2} \left( \frac{dX}{dt} \right)^2 + \frac{\partial^2 w}{\partial y^2} \left( \frac{dY}{dt} \right)^2 + 2 \frac{\partial^2 w}{\partial x \partial y} \left( \frac{dX}{dt} \right) \left( \frac{dY}{dt} \right) + 2 \frac{\partial^2 w}{\partial x \partial t} \left( \frac{dX}{dt} \right) \right. \right. \\ & \left. \left. + 2 \frac{\partial^2 w}{\partial y \partial t} \left( \frac{dY}{dt} \right) + \frac{\partial w}{\partial x} \left( \frac{d^2 X}{dt^2} \right) + \frac{\partial w}{\partial y} \left( \frac{d^2 Y}{dt^2} \right) \right]_{\substack{x \rightarrow X(t) \\ y \rightarrow Y(t)}} \right] \delta w = 0 \end{aligned} \tag{7}$$

Let  $w$  be interpolated by a series of the form

$$w = \sum_{j=1}^n A_j(t) \phi_j(x, y) \tag{8}$$

where,  $A_j$  denote the time-varying nodal amplitudes,  $\phi_j(x, y)$  are the boundary characteristic orthogonal polynomials and  $n$  is the number of the involved shape functions. Reproducing Eq. (7) with regard to Eq. (8) yields:

$$\mathbf{M}\ddot{\mathbf{A}} + \mathbf{C}\dot{\mathbf{A}} + \mathbf{K}\mathbf{A} = \mathbf{f} \tag{9}$$

wherein,

$$\begin{aligned} K_{ij} = & \int_0^A \int_0^B \left[ D \frac{\partial^2 \phi_i}{\partial x^2} \frac{\partial^2 \phi_j}{\partial x^2} + \nu D \left( \frac{\partial^2 \phi_i}{\partial x^2} \frac{\partial^2 \phi_j}{\partial y^2} + \frac{\partial^2 \phi_i}{\partial y^2} \frac{\partial^2 \phi_j}{\partial x^2} \right) + D \frac{\partial^2 \phi_i}{\partial y^2} \frac{\partial^2 \phi_j}{\partial y^2} + \frac{1}{3} Gh^3 \frac{\partial^2 \phi_i}{\partial x \partial y} \frac{\partial^2 \phi_j}{\partial x \partial y} \right] dx dy \\ & + M \zeta \phi_i \left[ \left( \frac{dX}{dt} \right)^2 \frac{\partial^2 \phi_j}{\partial x^2} + \left( \frac{dY}{dt} \right)^2 \frac{\partial^2 \phi_j}{\partial y^2} + \left( \frac{d^2 X}{dt^2} \right) \frac{\partial \phi_j}{\partial x} + \left( \frac{d^2 Y}{dt^2} \right) \frac{\partial \phi_j}{\partial y} + 2 \left( \frac{dX}{dt} \right) \left( \frac{dY}{dt} \right) \frac{\partial^2 \phi_j}{\partial x \partial y} \right]_{\substack{x \rightarrow X(t) \\ y \rightarrow Y(t)}} \end{aligned} \tag{10}$$

$$C_{ij} = 2M \zeta \phi_i \left[ \left( \frac{dX}{dt} \right) \frac{\partial \phi_j}{\partial x} + \left( \frac{dY}{dt} \right) \frac{\partial \phi_j}{\partial y} \right]_{\substack{x \rightarrow X(t) \\ y \rightarrow Y(t)}} \tag{11}$$

$$M_{ij} = \rho h \int_0^A \int_0^B \varphi_i \varphi_j dx dy + M \zeta \left[ \varphi_i \varphi_j \right]_{y \rightarrow Y(t)}^{x \rightarrow X(t)} \quad , \tag{12}$$

$$f_j = -Mg \left[ \varphi_j \right]_{y \rightarrow Y(t)}^{x \rightarrow X(t)} \quad . \tag{13}$$

Where, for moving mass problem  $\zeta = 1$  and in moving force case  $\zeta = 0$ .

### 2.1 Generating the BCOPs

The Gram-Schmidt algorithm is proposed herein to generate the BCOPs,  $\varphi_i(x, y)$ . The procedure is applied on a linearly independent set of the form:

$$F_i(x, y) = g(x, y) s_i(x, y), \quad i = 1, 2, 3, \dots \tag{14}$$

In which,

$$\begin{cases} s_i(x, y) \in \{1, x, y, x^2, xy, y^2, x^3, x^2y, xy^2, y^3, x^4, \dots\} \quad , \\ g(x, y) = x^o (1-x)^p y^q (1-y)^r \quad . \end{cases} \tag{15}$$

The plate boundary conditions are determined by assigning the values of 0, 1 or 2 to the parameters  $o, p, q$  and  $r$ . For clarity,  $p = 2$ , will force the plate edge at  $x = 1$  to be clamped;  $p = 1$  designates the side  $x = 1$  to be simply supported; and  $p = 0$  signifies that the side  $x = 1$  is free.  $g(x, y)$  satisfies the essential boundary conditions of the plate and  $s_i(x, y)$  are properly chosen linearly independent functions. The recursive Gram-Schmidt procedure can be applied according to

$$\begin{aligned} \phi_1(x, y) &= F_1(x, y), \\ \phi_i(x, y) &= F_i(x, y) - \sum_{j=1}^{i-1} \alpha_{ij} \phi_j(x, y), \end{aligned} \tag{16}$$

where, the constants  $\alpha_{ij}$  are specified by

$$\alpha_{ij} = \frac{\langle F_i(x, y), \phi_j(x, y) \rangle}{\langle \phi_j(x, y), \phi_j(x, y) \rangle} = \frac{\iint F_i(x, y) \phi_j(x, y) dx dy}{\iint \phi_j(x, y) \phi_j(x, y) dx dy} \tag{17}$$

### 2.2 Solution in Time Domain

The state- space representation of Eq. (9) could be expressed by:

$$\dot{\mathbf{X}}(t) = \boldsymbol{\beta}(t) \mathbf{X}(t) + \boldsymbol{\gamma}(t) \tag{18}$$

$$\begin{cases} \mathbf{X}(t) = \begin{bmatrix} \mathbf{A}(t) \\ \dot{\mathbf{A}}(t) \end{bmatrix}_{2n \times 1}, \\ \boldsymbol{\beta}(t) = \begin{bmatrix} \mathbf{0} & \mathbf{I} \\ -\mathbf{M}^{-1}\mathbf{K} & -\mathbf{M}^{-1}\mathbf{C} \end{bmatrix}_{2n \times 2n}, \\ \boldsymbol{\gamma}(t) = \begin{bmatrix} \mathbf{0} \\ \mathbf{M}^{-1}\mathbf{f} \end{bmatrix}_{2n \times 1}. \end{cases} \quad (19)$$

A solution to Eq. (18) could be achieved via matrix exponential:

$$\mathbf{X}(t) = \mathbf{Q}(t, \tau)\mathbf{X}(\tau) \quad (20)$$

$$\mathbf{Q}(t, \tau) \approx \mathbf{U}(t)\mathbf{U}^{-1}(\tau) \quad (21)$$

Where,  $\mathbf{U}$  is the fundamental solution matrix and  $\mathbf{Q}$  is a transfer matrix.

An approximation can be used to obtain  $\mathbf{Q}$  (Brogan, (1991)):

$$\mathbf{Q}(t_{k+1}, t_k) \approx e^{\boldsymbol{\beta}(t_k)\Delta t_k} \quad (22)$$

in which,  $\Delta t_k = t_{k+1} - t_k$  is the specified time step. Thus, Eq. (21) would easily be solved leading to:

$$\mathbf{X}(t_{k+1}) \approx e^{\boldsymbol{\beta}(t_k)\Delta t_k} \mathbf{X}(t_k) + [e^{\boldsymbol{\beta}(t_k)\Delta t_k} - \mathbf{I}]\boldsymbol{\beta}^{-1}(t_k)\boldsymbol{\gamma}(t_k) \quad (23)$$

### 3 NUMERICAL EXAMPLES

A steel plate with  $A(m) \times 2(m) \times 1(cm)$  dimensions and with the modulus of elasticity,

$E = 2.059 \times 10^{11} \text{ N/m}^2$ , mass density,  $\rho = 7850 \frac{\text{kg}}{\text{m}^3}$ , Poisson's ratio,  $\nu = 0.3$  is considered. Plate

aspect ratio,  $\alpha = \frac{A}{B}$  varies between 1 and 3 in the numerical examples and  $M_p = \rho hAB$  signifies

the plate mass. The moving mass travels along a rectilinear path on the plate's surface with different accelerations, velocities and weights. The rectilinear path lies on the center of the plate in  $y$  direction parallel to  $x$  axis as is depicted in Fig. 1-(a), that is:

$$\begin{cases} X(t) = \frac{1}{2}at^2 + v_0t, \\ Y(t) = \frac{b}{2}. \end{cases} \quad (24)$$

In which,  $a$  is the constant acceleration, and  $v_0$  is the initial velocity of the moving mass. Four different boundary conditions according to Fig. 1-(b) have been chosen for the implementation of the analyses, SSSS, CCCC, SFSF and CFFF.

### 3.1 Validation

Intended in Tables 1 and 2 respectively for  $\alpha = 1.0$  and  $\alpha = 2.0$  are giving a measure of convergence rate and error estimation according to the exact solution (Leissa, (1973)). To this end, the computational error percentage of the plate natural frequencies in comparison with their exact values is indicated. It is evident that increasing the number of involved BCOPs improves precision. From an engineering practitioner stand point it can be noted that involving more than 25, 36, 49, 64 and 81 shape functions do not cause a noticeable improvement for the first, 4<sup>th</sup>, 9<sup>th</sup>, 16<sup>th</sup> and 25<sup>th</sup> natural frequencies, correspondingly.

Assumed mode shapes	25	36	49	64	81
frequency					
first	2.65E-05	2.96E-08	1.16E-11	1.51E-12	6.59E-12
4th	0.137562	0.008236	5.28E-05	8.3E-07	1.66E-07
9th	3.917068	0.12875	0.00172	0.00165	9.84E-06
16th	42.68562	7.765838	0.438665	0.010594	0.000128
25th	246.8608	73.07376	27.63008	13.67999	3.853367

Table 1: - Error percentage of the frequencies for the plate with  $\alpha = 1.0$  and SSSS boundary condition.

Assumed mode shapes	25	36	49	64	81
frequency					
first	4.46927E-05	3.32131E-08	9.71906E-12	6.96837E-13	8.06322E-13
4th	0.002292011	5.03986E-06	5.03682E-06	5.59054E-09	3.33709E-12
9th	2.85186715	2.850895044	0.141149617	0.00306609	0.002739483
16th	72.74046477	25.16953101	9.953054093	1.001344734	0.479836497
25th	336.131711	75.93077998	8.797073947	7.646938583	0.668243947

Table 2: - Error percentage of the frequencies for the plate with  $\alpha = 2.0$  and SSSS boundary condition.

In this article, the DAF for SSSS, CCCC and SFSF boundary conditions refers to the maximum plate center point dynamic response divided into the corresponding maximum static deformation. In the case of a cantilever plate, the midpoint of the plate free edge at  $x = A$  is the reference point for capturing the DAF. Moreover, a velocity type parameter  $v' = \frac{2A}{T_1}$  is introduced herein to ac-

complish normalization, in which,  $T_1$  is the first natural period of the plate. The first 36 BCOPs are taken into account and both the moving force, and the moving mass are included. To examine the validity of calculations, the DAF spectra for a simply supported plate is exported by the present approach and compared with the benchmark solution provided via eigenfunction expansion method by Nikkhoo and Rofooei (2012) in Fig. 2, wherein, an excellent agreement can be realized. Nikkhoo Latin American Journal of Solids and Structures 12 (2015) 317-332



and Rofooei (2012) have provided the curves employing the first 25 natural shape functions of the plate. They mentioned that mode-shapes higher than 25 do not have a significant contribution. In view of the preceding, inclusion of the first 36 BCOPs seems to be sufficient enough to conduct the current study without a remarkable loss of precision within the scale of the diagrams.

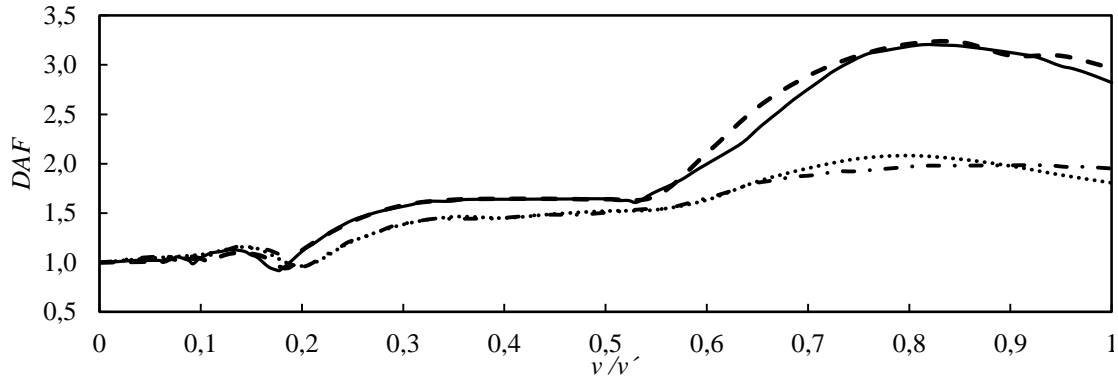


**Figure 2:** DAF spectra of a simply supported plate ( — moving mass (Nikkhoo and Rofooei ,(2012)), - - - moving force(Nikkhoo and Rofooei ,(2012)), --- present study moving mass, ... present study moving force)  $M = 0.15M_p$ ,  $\alpha = 2.0$ ,  $a = 0$ .

### 3.2 Parametric Studies

Most of the previously carried out parametric investigations have confined their findings by merely considering the case of a simply supported plate and the issue is open to discuss for other plate fixities. In Fig. 3, the DAF of the plate is displayed versus the initial velocity for the boundary conditions of SSSS, CCCC, SFSS and CFFF. Moving mass weight ratio within  $M/M_p = 0.05$  up to  $M/M_p = 0.2$  is regarded to cover a practical range of inertia. For the SSSS, CCCC and SFSS plate fixities, a similar pattern of DAF spectra is evident and the lower/upper bound curves correspond to the lower/higher load inertia. However, sensitivity of the plate response to the variation of load inertia in SFSS boundary condition is less than SSSS and CCCC. Moving to the CFFF plate, a substantially disparate scheme of DAF change can be seen. In the preceding case, the heavier load produces the lower amplitude of vibration even featuring below unit values. To elucidate, a benchmark time history of the cantilever plate at its free edge is depicted in Fig. 4, where the moving force framework observed to overestimate the plate response due to a moving mass. Accordingly, the boundary condition of the plate seems to be a key parameter in the dynamic behavior of a plate under a moving mass that can no longer be neglected. Hence, the contribution of plate fixity is taken into account in Figs. 5, 6, 7 and 8. As a general rule, by increasing the mass weight and velocity of the moving force, it is like the base structural natural frequency is virtually decreasing because of the inertial effects. Therefore, the response of the structure under a moving mass increases in most of the cases where the base plate behaves as a softer structure in comparison with the moving load excitation (this fact is not true for the CFFF boundary condition (Kiani et al. (2009a)).

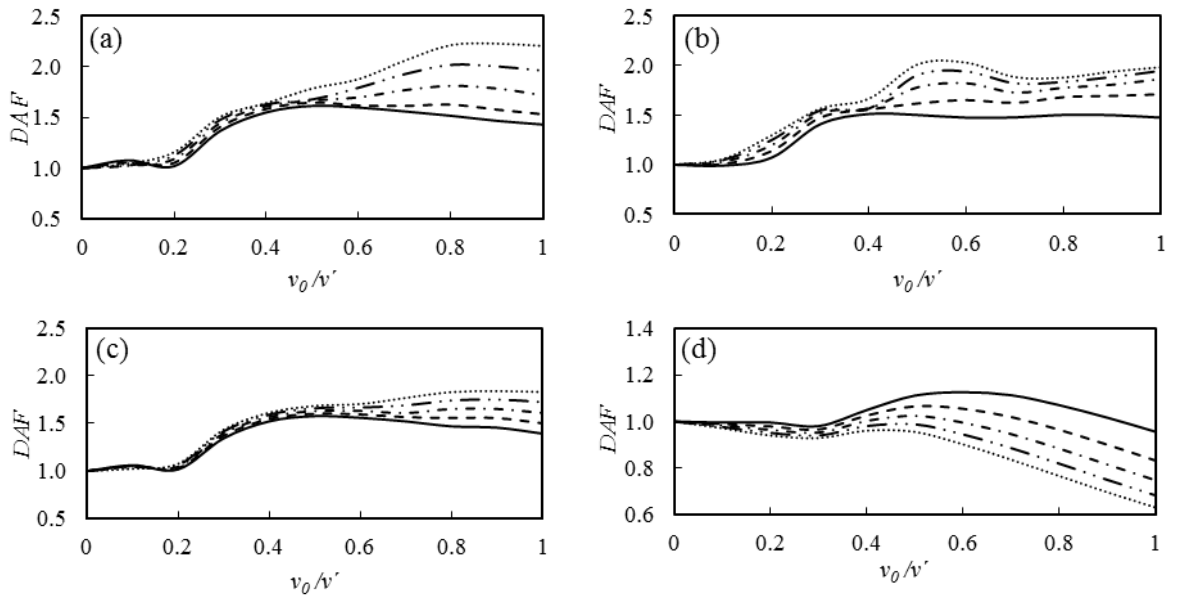


Figure 3: The effects of the moving load velocity and plate boundary conditions on the DAF for  $\alpha = 1.0$  and  $\alpha = 0$ . (a) SSSS, (b) CCCC, (c) SFSF, (d) CFFF. (— moving force, ---  $M = 0.05M_P$ , -.-  $M = 0.1M_P$ , -.-.-  $M = 0.15M_P$ , ...  $M = 0.2M_P$ ).

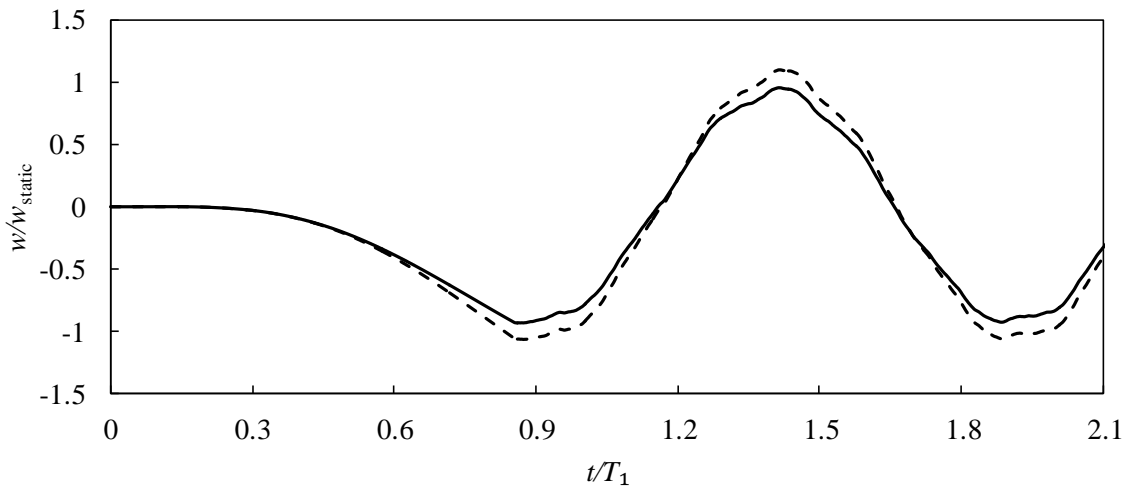


Figure 4: Time history of a cantilever plate dynamic response captured at  $x = A$ ,  $y = 0.5B$ ;  $v_0 = 0.5v^*$ ,  $a = 0.4a^*$ ,  $\alpha = 1.0$ ,  $M = 0.15M_P$ . (—moving mass, --- moving force).

The effects of the plate aspect ratio parameter have been recently assessed by Nikkhoo and Rofooei (2012) while only the case of a SSSS plate has been focused. In case of a cantilever plate, it is observed herein that the aspect ratio does not cause sensible influence on the plate maximum DAF. In Latin American Journal of Solids and Structures 12 (2015) 317-332

Fig.5, the maximum DAF extracted from SSSS and CCCC boundary conditions cover a range of 1.5 to 4.5 considering a variation of the aspect ratio between 1 and 3. According to the Fig.5, the SSSS case shows a rather faster rate of the maximum DAF variation with respect to the aspect ratio change in comparison with the CCCC and SF/SF cases.

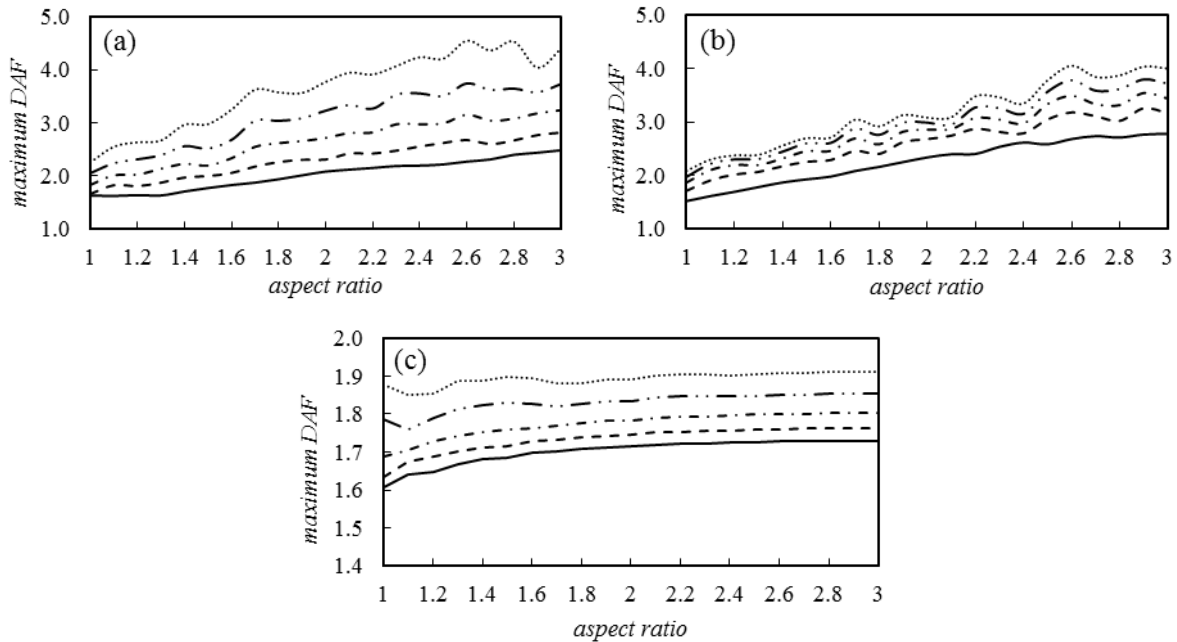


Figure 5: The effects of the moving load velocity and plate boundary conditions on the maximum DAF for  $\alpha = 0$ ,  $v \leq v'$ . (a) SSSS, (b) CCCC, (c) SF/SF, (— moving force, ---  $M = 0.05M_P$ , - - -  $M = 0.1M_P$ , - . . -  $M = 0.15M_P$ , ...  $M = 0.2M_P$ )

In Fig .6, one can clearly distinguish the noticeable diversity of an accelerated motion comparing it to a non-accelerated one (Nikkhoo and Rofooei ,(2012); Vaseghi Amiri et al.(2013);Rofooei and Nikkhoo(2009)).The general pattern of the DAF variation against the initial velocity is very similar in the SSSS and SF/SF cases in Fig. 6. With a more optimistic point of view, the CCCC plate also seems to have the same manner as that of SSSS and SF/SF. However, the cantilever plate demonstrates a quite different behavior. The DAF decreases with the growth of initial velocity in the case of the CFFF in spite of the other assumed boundary conditions.

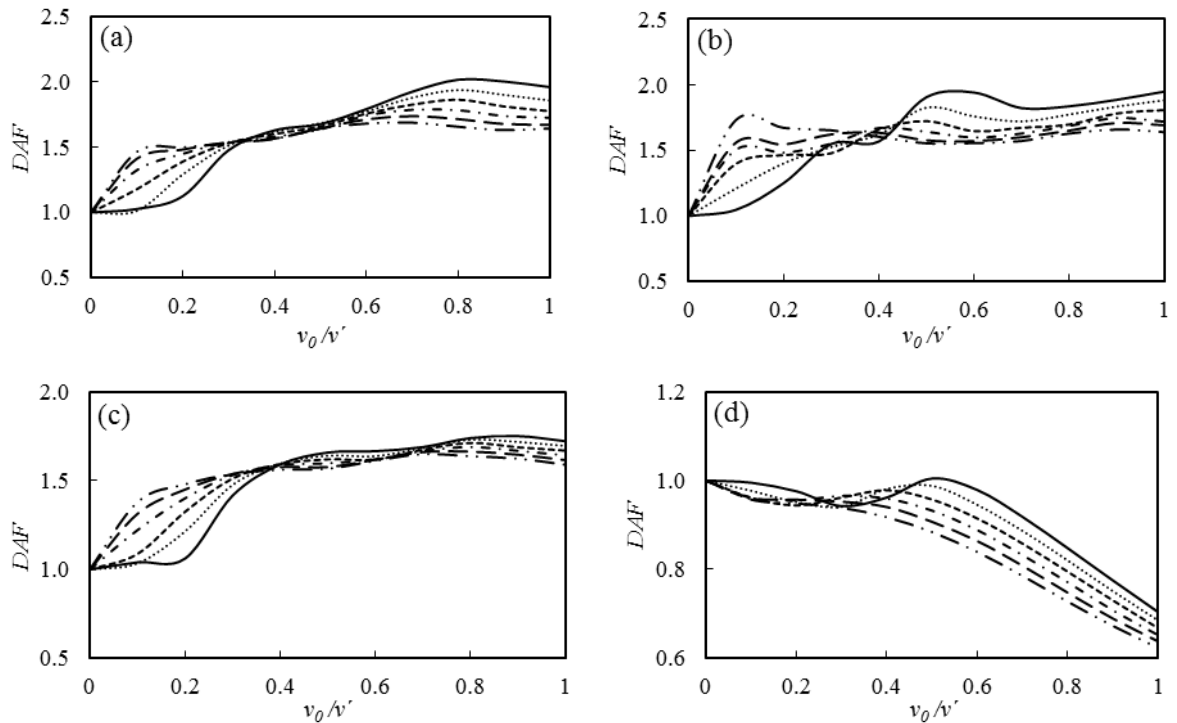


Figure 6: The effects of the moving mass initial velocity and plate boundary conditions on the DAF for  $\alpha = 1.0$  and  $M = 0.15M_p$ ; (a) SSSS, (b) CCCC, (c) SFSF, (d) CFFF. (—  $a = 0$ , ...  $a = 0.2a'$ , - -  $a = 0.4a'$ , - . -  $a = 0.6a'$ , - - -  $a = 0.8a'$  and - . . -  $a = 1.0a'$ )

The effect of load acceleration and inertia is illustrated in Fig.7.  $a' = A/T_1^2$  is an acceleration parameter to perform the normalization of the acceleration data. The analyses feature a descending manner of the maximum DAF change as the acceleration grows larger in most of the cases with a reasonable engineering precision. Furthermore, for a specific acceleration value, it can be seen that increasing the inertia of the moving force leads to smaller amplitude of vibration.

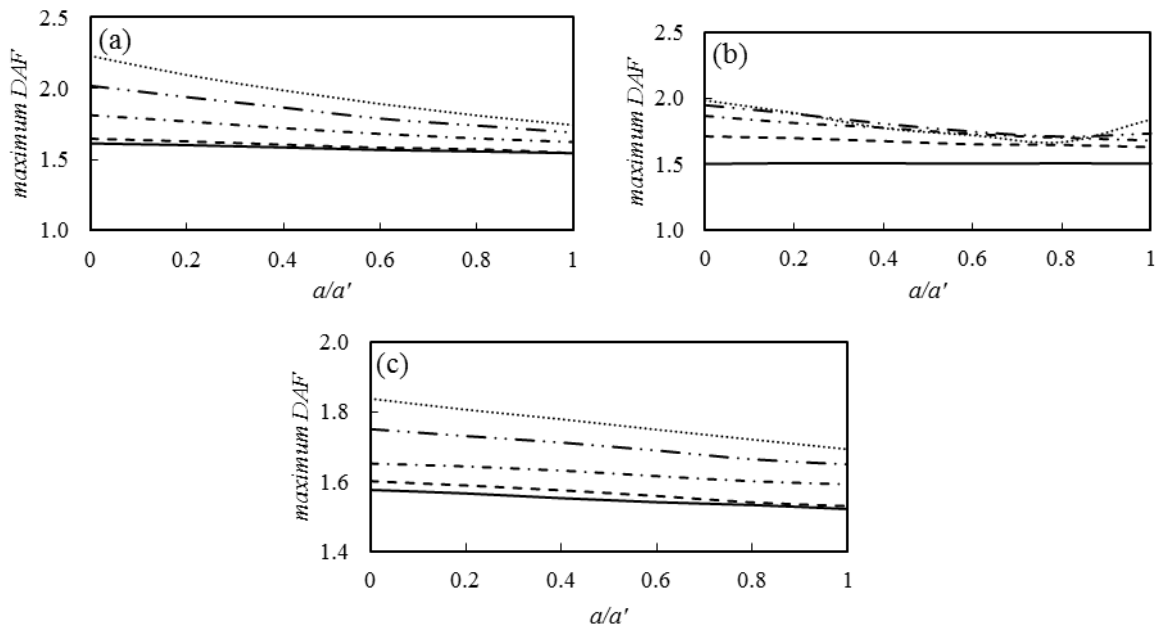


Figure 7: The effects of the moving load acceleration and plate boundary conditions on the maximum DAF for  $\alpha = 1.0$ ,  $v \leq v'$ ; (a) SSSS, (b) CCCC, (c) SFSF. (— moving force, ---  $M = 0.05M_P$ , -.-  $M = 0.1M_P$ , - - -  $M = 0.15M_P$ , ...  $M = 0.2M_P$ )

The maximum DAF values are plotted against the plate aspect ratio for different magnitudes of moving mass acceleration in Fig. 8, which yields to even better understanding of the role of load traversing acceleration and the plate boundary conditions. A clear alteration in the plate dynamic behavior pattern can be contrasted for the SSSS, CCCC and the SFSF cases. In the CCCC plate, the maximum DAF shows a more sensitivity rather than SSSS and SFSF with more irregularity. The maximum DAF ascends with the growth of aspect ratio in the case of CCCC regarding  $a = 0.2a'$  and  $a = 0.4a'$ , however, for  $a \geq 0.6a'$  two phases could be observed. The maximum DAF increases and after reaching a peak value decreases as the aspect ratio gets larger. In the case of the SFSF fixity, a relatively regular manner could be observed. For all of the acceleration values, the maximum DAF increases with the growth of aspect ratio considering  $\alpha \geq 1.2$ . Besides, for both SSSS and SFSF cases, the maximum DAF grows as the acceleration rises corresponding to a given aspect ratio except for  $a = a'$  in case of the SSSS plate.

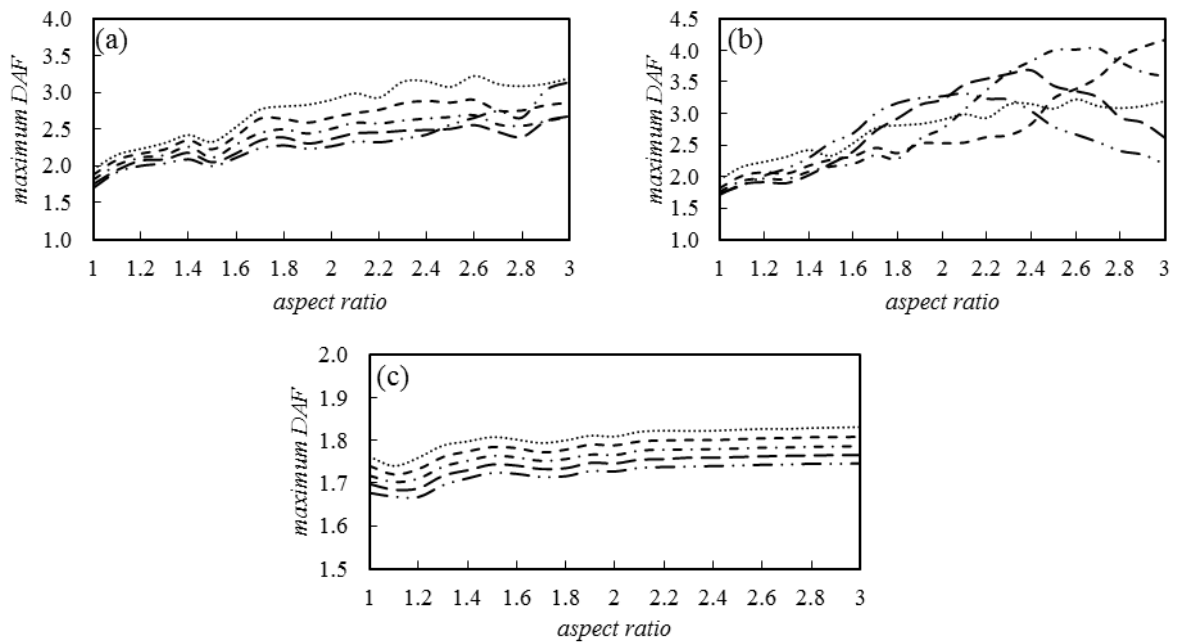


Figure 8: The effects of the plate aspect ratio and boundary conditions on the DAF for  $M = 0.15M_P$  and  $v \leq v'$ ; (a) SSSS, (b) CCCC, (c) SFSS, (d) CFFF. ( ...  $a = 0.2a'$ , ---  $a = 0.4a'$ , -.-  $a = 0.6a'$ , - - -  $a = 0.8a'$ , - . . . -  $a = 1.0a'$  )

## 4 CONCLUSIONS

The classical plate theory is utilized to achieve dynamics of an isotropic undamped rectangular plate due to an accelerating moving mass. BCOPs are used as the computational approach to obtain the solutions which show a rapid convergence rate regarding the number of the involved orthogonal shape functions. Four different boundary conditions, i.e., SSSS, CCCC, SFSS and CFFF are scrutinized in the numerical examples. Parametric evaluation of the plate DAF was widely performed accounting for a broad range of the parameter's variation to explore the effects of the moving mass acceleration, initial velocity, weight and plate's aspect ratio on the plate DAF. The following observations could be highlighted according to the presented study:

- The application of at least 36 BCOPs seems to be adequate to accomplish sufficiently precise computation desired by an engineering practitioner.
- In switching between different plate boundary conditions, the method of BCOPs is more flexible and convenient with respect to the eigenfunction expansion method. BCOPs can handle all possible 21 combinations of S, C and F classical boundary conditions of a rectangular plate demanding just simple manipulation of splines. While in the modal analysis, the theorem is mathematically quite general but in practice, analytical solution of thin rectangular plate, free vibration only exists for 6 boundary conditions (Leissa (1973) Leissa and Qatu, (2011)). It should be empha-

sized that in the case of non-simply supported plates, the closed-form solution of free vibration becomes more complex, which is not favorable for an engineering practitioner.

- The accelerating traveling mass can lead to substantially different patterns of plate dynamic behavior that may not appear in a non-accelerating case.
- Consideration of plate boundary condition is an important governing factor in the determination of the plate vibration due to a traveling inertial load.

## References

- Ahmadi, M., Nikkhoo, A. (2014). "Utilization of characteristic polynomials in vibration analysis of non-uniform beams under a moving mass excitation" , *Applied Mathematical Modelling*, 38(7), pp. 2130-2140.
- Awodola, T. O., and S. T. Oni. (2013). "Dynamic response to moving masses of rectangular plates with general boundary conditions and resting on variable Winkler foundation" , *Latin American Journal of Solids and Structures* , 10(2), pp. 301-322.
- Bhat, R.B. (1985). "Natural frequencies of rectangular plates using characteristic orthogonal polynomials in Rayleigh-Ritz method", *Journal of Sound and Vibration*, 102(4), pp. 493-499.
- Brogan, W.L. (1991) "Modern control theory", Prentice-Hall, New Jersey.
- Bulut, H. and Kelesoglu, O. (2010). "Comparing numerical methods for response of beams with moving mass", *Advances in Engineering Software*, 41(7-8), pp. 976-980.
- Chakraverty, S.(1992). "Numerical solution of vibration of plates", PhD Thesis, University of Roorkee (Now IIT, Roorkee), Roorkee, India.
- Cifuentes, A. and Lalapet, S. (1992). "A general method to determine the dynamic response of a plate to a moving mass", *Computers & Structures*, 42(1), pp. 31-36.
- De Faria, A.R. and Oguamanam, D.C.D. (2004) "Finite element analysis of the dynamic response of plates under traversing loads using adaptive meshes", *Thin-Walled Structures*, 42(10), pp. 1481-1493.
- Ebrahimzadeh Hassanabadi, M., Nikkhoo, A., Vaseghi Amiri, J. and Mehri, B. (2013) "A new Orthonormal Polynomial Series Expansion Method in vibration analysis of thin beams with non-uniform thickness", *Applied Mathematical Modeling*, 37(18-19), pp. 8543-8556.
- Ebrahimzadeh Hassanabadi, M., Vaseghi Amiri, J., Davoodi M.R. (2014a) "On the vibration of a thin rectangular plate carrying a moving oscillator", *Scientia Iranica, Transaction A: Civil Engineering*, 21(2), pp. 284-294.
- Ebrahimzadeh Hassanabadi, M., Khajeh Ahmad Attari, N., Nikkhoo, A., Baranadan, M. (2014b) "An optimum modal superposition approach in the computation of moving mass induced vibrations of a distributed parameter system", *Proceedings of the Institution of Mechanical Engineers, Part C: Journal of Mechanical Engineering Science*, DOI: 10.1177/0954406214542968.
- Eftekhari Azam, S., Mofid, M. and Afghani Khoraskani, R. (2013). "Dynamic response of Timoshenko beam under moving mass", *Scientia Iranica, Transactions A: Civil Engineering*, 20(1), pp. 50-56.
- Esen, İ. (2013) "A new finite element for transverse vibration of rectangular thin plates under a moving mass", *Finite Elements in Analysis and Design*, 66, pp. 26-35.
- Fryba, L. (1999) "Vibration of Solids and Structures under Moving Loads", Thomas Telford, London.
- Ghafoori, E., Kargarnovin, M.H. and Ghahremani, A.R. (2011). "Dynamic responses of a rectangular plate under motion of an oscillator using a semi-analytical method", *Journal of Vibration and Control*, 17(9), pp. 1310-1324.
- Kiani, K., Nikkhoo, A. and Mehri, B. (2009a). "Prediction capabilities of classical and shear deformable beam models excited by a moving mass", *Journal of Sound and Vibration*, 320, pp. 632-648.
- Kiani, K., Nikkhoo, A. and Mehri, B. (2009b). "Parametric analyses of multispan viscoelastic shear deformable beams under excitation of a moving mass", *Journal of Vibration and Acoustics*, 131(5), pp. 051009(1-12).

- Kiani, K., Nikkhoo, A. and Mehri, B. (2010). "Assessing dynamic response of multispan viscoelastic thin beams under a moving mass via generalized moving least square method", *Acta Mechanica Sinica*, 26(5), pp. 721-733.
- Kiani, K., Nikkhoo, A. (2012). "On the limitations of linear beams for the problems of moving mass-beam interaction using a mesh free method", *Acta Mechanica Sinica*, 28(1), pp. 164-179.
- Lee, U. (1996). "Revisiting the moving mass problem: onset of separation between the mass and beam", *Journal of Vibration and Acoustic*, 118(3), 516 - 521.
- Leissa, A.W. (1973). "The free vibration of rectangular plates", *Journal of Sound and Vibration*, 31(3), pp. 257-293.
- Leissa, A.W. and Qatu, M.S. (2011). "Vibration of Continuous Systems", McGraw Hill, NY.
- Liew, KM., Lam, KY. and Chow, ST. (1990) "Free vibration analysis of rectangular plates using orthogonal plate function", *Computers & Structures*, 34(1), 79-85.
- Mohebpour, S.R., Malekzadeh, P. and Ahmadzadeh, A.A. (2011). "Dynamic analysis of laminated composite plates subjected to a moving oscillator by FEM", *Composite Structures*, 93(6), pp. 1574-1583.
- Nikkhoo, A., Rofooei, F.R. and Shadnam, M.R. (2007). "Dynamic behavior and modal control of beams under moving mass", *Journal of Sound and Vibration*, 306 (3 - 5), pp. 712 - 724.
- Nikkhoo, A. and Rofooei, F.R. (2012). "Parametric study of the dynamic response of thin rectangular plates traversed by a moving mass", *Acta Mechanica*, 223(1), pp. 15-27.
- Nikkhoo, A., Ebrahimzadeh Hassanabadi, M., Eftekhari Azam, S., Vaseghi Amiri, J. (2014). "Vibration of a thin rectangular plate subjected to series of moving inertial loads", *Mechanics Research Communications*, 55, pp. 105-113.
- Nikkhoo, A. Farazandeh A., Ebrahimzadeh Hassanabadi M., Mariani S., "Simplified modeling of beam vibrations induced by a moving mass through regression analysis", *Acta Mechanica*, DOI 10.1007/s00707-015-1309-3.
- Olsson, M. (1991). "On the fundamental moving load problem", *Journal of sound and vibration*, 145(2), pp. 299-307.
- Oni, S. T., and T. O. Awodola. (2011). "Dynamic behaviour under moving concentrated masses of simply supported rectangular plates resting on variable Winkler elastic foundation." *Latin American Journal of Solids and Structures* 8.4: 373-392.
- Ouyang, H. (2011). "Moving load dynamic problems: A tutorial (with a brief overview)", *Mechanical Systems and Signal Processing*, 25(6), pp. 2039-2060 .
- Rofooei, F.R. and Nikkhoo, A. (2009). "Application of active piezoelectric patches in controlling the dynamic response of a thin rectangular plate under a moving mass", *International Journal of Solids and Structures*, 46(11-12), pp. 2429-2443.
- Shadnam, M.R., Mofid, M. and Akin, J.E. (2001). "On the dynamic response of rectangular plate, with moving mass", *Thin-Walled Structures*, 39(9), pp. 797-806.
- Singh, B. and Chakraverty, S. (1994). "Boundary characteristic orthogonal polynomials in numerical approximation", *Communications in numerical methods in engineering*, 10(12), 1027-1043.
- Stăncioiu, D., Ouyang, H. and Mottershead, J.E. (2008). "Vibration of a beam excited by a moving oscillator considering separation and reattachment", *Journal of Sound and Vibration*, 310(4 - 5) 1128 - 1140.
- Vaseghi Amiri, J., Nikkhoo, A., Davoodi, M.R. and Ebrahimzadeh Hassanabadi, M. (2013). "Vibration analysis of a Mindlin elastic plate under a moving mass excitation by eigenfunction expansion method", *Thin-Walled Structures*, 62, pp. 53-64 .
- Wu, J.J. (2003). "Vibration of a rectangular plate undergoing forces moving along a circular path", *Finite Elements in Analysis and Design*, 40(1), pp. 41-60.
- Wu, J.J. (2005). "Dynamic analysis of a rectangular plate under a moving line load using scale beams and scaling laws", *Computers and Structures*, 83(19-20), pp. 1646-1658.
- Zarfam, R., Khaloo, A.R. and Nikkhoo, A. (2013). "On the response spectrum of Euler - Bernoulli beams with a moving mass and horizontal support excitation", *Mechanics Research Communications*, 47, pp. 77 - 83.